Article

Polymer–DNA Hybrids as Electrochemical Probes for the Detection of DNA

Julianne M. Gibbs, So-Jung Park, Donde R. Anderson,
Keith J. Watson, Chad A. Mirkin, and SonBinh T. Nguyen

J. Am. Chem. Soc., **2005**, 127 (4), 1170-1178• DOI: 10.1021/ja046931i • Publication Date (Web): 07 January 2005

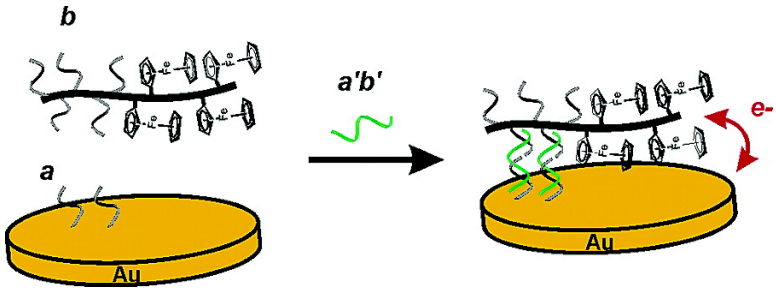

More About This Article

Additional resources and features associated with this article are available within the HTML version:

- Supporting Information
- Links to the 20 articles that cite this article, as of the time of this article download
- Access to high resolution figures
- Links to articles and content related to this article
- Copyright permission to reproduce figures and/or text from this article

View the Full Text HTML

J|A|C|S
ARTICLES
Published on Web 01/07/2005

Polymer−DNA Hybrids as Electrochemical Probes for the Detection of DNA

Julianne M. Gibbs, So-Jung Park, Donde R. Anderson, Keith J. Watson, Chad A. Mirkin,* and SonBinh T. Nguyen*

Contribution from the Department of Chemistry and Institute for Nanotechnology, Northwestern University, 2145 Sheridan Road, Evanston, Illinois 60208-3113

Received May 25, 2004; E-mail: chadnano@northwestern.edu; stn@northwestern.edu

Abstract: The syntheses of several norbornene block copolymers containing oligonucleotide and ferrocenyl side chains and their use in the electrochemical detection of DNA are described. Two kinds of DNA-containing block copolymers with either ferrocenyl or dibromoferrocenyl groups were prepared via ring-opening metathesis polymerization (ROMP). Based on these two distinct ferrocene derivatives, a triblock copolymer labeling strategy was developed. With this strategy, the identity of DNA target can be determined by the $E_{1/2}$s of the ferrocenyl moieties and the ratio of peak currents. These polymers exhibit predictable and tailorable electrochemical properties, high DNA duplex stability, and unusually sharp melting transitions, which are highly desirable characteristics for DNA detection applications. Significantly, single-base mismatches could be easily detected using two distinct block copolymers as dual-channel detection probes in an electrochemical DNA detection format.

Introduction

During the past few years there has been growing interest in the synthesis and utilization of nanostructured materials in which multiple DNA strands of known sequence are attached to a central "core". These materials include oligonucleotide-modified gold nanoparticles and oligonucleotide-functionalized dendrimers.[1−4] These particular materials have been utilized in a number of DNA detection applications,[4−9] and their novel properties have led to major advantages with respect to sensitivity, selectivity, ease of data readout and analysis, and even cost. For example, in the case of the oligonucleotide-modified gold nanoparticles, many (over 100) thiol-modified DNA strands are attached to the surface of citrate-stabilized gold nanoparticles via a ligand exchange process.[1,10] The resulting oligonucleotide-modified nanoparticles after complexation with other nanoparticles that have been modified with complementary oligonucleotide sequences exhibit extraordinarily sharp melting profiles. Recognition and application of this cooperative behavior in several DNA detection systems have led to significant improvements in the selectivities of such assays.[7−9] In addition, both the dendrimer- and nanoparticle-based strategies have led to novel signal amplification strategies, which have improved the sensitivity of assays based upon them by many orders of magnitude when compared with molecular fluorophore probe technologies.[4,8,9]

Recently, we reported a methodology for chemically attaching multiple DNA strands to well-defined ROMP-based (ROMP = ring-opening metathesis polymerization)[11] organic polymers and block copolymers of norbornene derivatives (Scheme 1).[12] In this approach, the metathesis catalyst $Cl_2(PPh_3)_2Ru{=}CHPh$ (**1**) was used to polymerize a novel norbornenyl monomer containing a diphenylacetylene-benzyl alcohol spacer (**2**). Post-polymerization modification of the resulting polymer with 2-cyanoethyl tetraisopropylphosphorodiamidite (**3**) led to the isolation of a polymer that can be readily coupled to DNA using standard solid-phase synthesis techniques.[13] Significantly, ROMP-based polymers modified with complementary oligonucleotide strands reversibly hybridized to form aggregates with very sharp "melting" characteristics similar to those observed in the oligonucleotide-modified gold nanoparticle systems.[1,10]

Due to the living nature of ROMP catalyzed by **1** and its functional group tolerance, a wide variety of functional groups can be incorporated into ROMP-based polymer−DNA hybrid structures in a highly tailorable and controlled manner, allowing one to encode such structures with identification "tags". These hybrids can then be used to build materials with recognition

(1) Mirkin, C. A.; Letsinger, R. L.; Mucic, R. C.; Storhoff, J. J. *Nature* **1996**, *382*, 607−609.
(2) Shchepinov, M. S.; Dalova, A. U.; Bridgman, A. J.; Southern, E. M. *Nucleic Acids Res.* **1997**, *25*, 4447−4454.
(3) Shchepinov, M. S.; Mir, K. U.; Elder, J. K.; Frank-Kamenetskii, M. D.; Southern, E. M. *Nucleic Acids Res.* **1999**, *27*, 3035−3041.
(4) Collins, M. L.; Irvine, B.; Tyner, D.; Fine, E.; Zayati, C.; Chang, C.; Horn, T.; Ahle, D.; Detmer, J.; Shen, L.-P.; Kolberg, J.; Bushnell, S.; Urdea, M. S.; Ho, D. D. *Nucleic Acids Res.* **1997**, *25*, 2979−2984.
(5) Elghanian, R.; Storhoff, J. J.; Mucic, R. C.; Letsinger, R. L.; Mirkin, C. A. *Science* **1997**, *277*, 1078−1081.
(6) Storhoff, J. J.; Elghanian, R.; Mucic, R. C.; Mirkin, C. A.; Letsinger, R. L. *J. Am. Chem. Soc.* **1998**, *120*, 1959−1964.
(7) Taton, T. A.; Mirkin, C. A.; Letsinger, R. L. *Science* **2000**, *289*, 1757−1760.
(8) Taton, T. A.; Lu, G.; Mirkin, C. A. *J. Am. Chem. Soc.* **2001**, *123*, 5164−5165.
(9) Park, S.-J.; Taton, T. A.; Mirkin, C. A. *Science* **2002**, *295*, 1503−1506.
(10) Demers, L. M.; Mirkin, C. A.; Mucic, R. C.; Reynolds, R. A.; Letsinger, R. L.; Elghanian, R.; Viswanadham, G. *Anal. Chem.* **2000**, *72*, 5535−5541.
(11) Trnka, T. M.; Grubbs, R. H. *Acc. Chem. Res.* **2001**, *34*, 18−29.
(12) Watson, K. J.; Park, S.-J.; Nguyen, S. T.; Mirkin, C. A. *J. Am. Chem. Soc.* **2001**, *123*, 5592−5593.
(13) Brown, T.; Brown, D. J. S. in *Oligonucleotides and Analogues*; Eckstein, F., Ed.; Oxford University Press: New York, 1991.

10.1021/ja046931i CCC: $30.25

Scheme 1. Synthesis of Polymer−DNA Hybrids

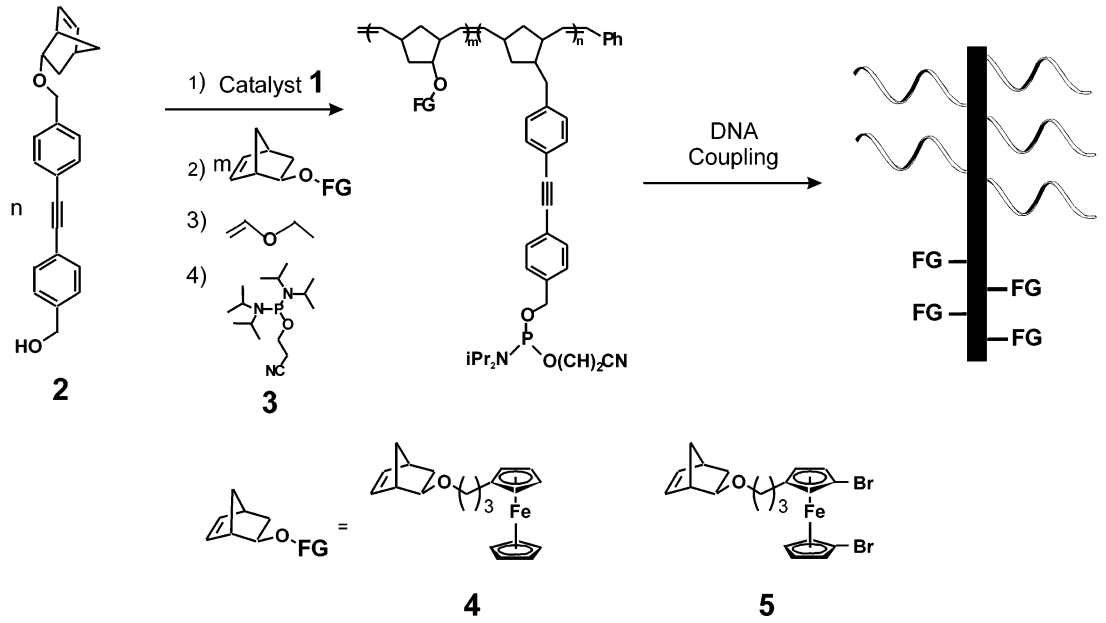

capabilities and other physical properties and as probes in novel detection systems. Herein, we demonstrate the generality and the utility of this hybrid polymer−DNA approach in a scheme for the electrochemical detection of DNA. Specifically, we have synthesized both diblock and triblock copolymers of oligonucleotides and ferrocene derivatives **4** and **5** and characterized their electrochemical and DNA hybridization properties. The diblock copolymers were then used successfully in the electrochemical detection[14−19] of pM-levels of oligonucleotides where the presence of an electrochemical signal after DNA hybridization signifies the presence of a target strand (vide infra). With two different diblock copolymer−DNA probes, small differences in DNA sequence mismatches (single-base pair) can be reliably distinguished. When using a triblock copolymer−DNA hybrid with two ferrocene blocks possessing widely spaced redox potentials, the number of polymer−DNA electrochemical signaling probes can be significantly increased by tailoring the peak positions and the intensity ratios of the ferrocene blocks, allowing one to detect multiple targets simultaneously and accurately.

Although most commercially available detection systems use fluorescence spectroscopy, numerous electrochemically based sensing methods have been reported in recent years. The interest in electrochemical detection stems from the simplicity of the required voltammetric instrumentation as well as its potential for miniaturization and use in point-of-care assays.[18,19] The electrochemical component of these detection schemes varies widely; some systems rely on DNA intercalators, the direct oxidation of nucleotides, or signal amplification based on enzymatic processes. Other approaches have employed oligonucleotides covalently modified with redox-active small molecules[20] in strategies similar to fluorescent-based molecular probe assays.[16,17,21−28] When compared with these electrochemically active molecular probes, the block copolymers reported herein exhibit several desirable DNA hybridization properties such as larger binding constants (manifested in higher T_m) and sharper melting transitions which lead to better target differentiation capabilities (vide infra) and higher sensitivities. As a basis for comparison, we developed a molecular probe that is structurally similar to a repeating unit of our polymer probe and acquired a series of melting profiles to further evaluate and substantiate the advantages of our ROMP polymer-based systems.

Results and Discussion

Syntheses of Diblock Copolymer−DNA Hybrids. Block copolymer hybrids (**Hybrid I**−**Hybrid IV**) of DNA and redox-active molecules (**4**, **5**) were synthesized by attaching oligonucleotides to the preformed ROMP polymers (Scheme 1). Each block copolymer was synthesized by reacting the DNA-modifiable monomer **2** with Grubbs catalyst **1** until all of the monomer had been consumed and then polymerizing either monomer **4** or **5**, followed by termination with ethyl vinyl ether, to yield diblock copolymers poly**2**-poly**4** and poly**2**-poly**5**, respectively. These polymer precursors were then coupled to the 5′ end of oligonucleotides to yield **Hybrid I**−**Hybrid IV**

(14) Kelley, S. O.; Boon, E. M.; Barton, J. K.; Jackson, N. M.; Hill, M. G. *Nucleic Acids Res.* **1999**, *27*, 4830−4837.
(15) Napier, M. E.; Loomis, C. R.; Sistare, M. F.; Kim, J.; Eckhardt, A. E.; Thorp, H. H. *Bioconjugate Chem.* **1997**, *8*, 906−913.
(16) Ihara, T.; Maruo, Y.; Takenaka, S.; Takagi, M. *Nucleic Acids Res.* **1996**, *24*, 4273−4280.
(17) Yu, C. J.; Wan, Y.; Yowanto, H.; Li, J.; Tao, C. L.; James, M. D.; Tan, C. L.; Blackburn, G. F.; Meade, T. J. *J. Am. Chem. Soc.* **2001**, *123*, 11155−11161.
(18) Wang, J. *Anal. Chim. Acta* **2002**, *469*, 63−71.
(19) Drummond, T. G.; Hill, M. G.; Barton, J. K. *Nat. Biotechnol.* **2003**, *21*, 1192−1199.
(20) Immoos, C. E.; Lee, S. J.; Grinstaff, M. W. *J. Am. Chem. Soc.* **2004**, *126*, 10814−10815.
(21) Brazill, S. A.; Kim, P. H.; Kuhr, W. G. *Anal. Chem.* **2001**, *73*, 4882−4890.
(22) Brazill, S. A.; Kuhr, W. G. *Anal. Chem.* **2002**, *74*, 3421−3428.
(23) Brazill, S.; Hebert, N. E.; Kuhr, W. G. *Electrophoresis* **2003**, *24*, 2749−2757.
(24) Yu, C. J.; Wang, H.; Wan, Y.; Yowanto, H.; Kim, J. C.; Donilon, L. H.; Tao, C.; Strong, M.; Chong, Y. *J. Org. Chem.* **2001**, *66*, 2937−2942.
(25) Cosnier, S.; Gondran, C.; Dueymes, C.; Simon, P.; Fontecave, M.; Decout, J.-L. *Chem. Commun.* **2004**, 1624−1625.
(26) Kim, K.; Yang, H.; Park, S. H.; Lee, D.-S.; Kim, S.-J.; Lim, Y. T.; Kim, Y. T. *Chem. Commun.* **2004**, 1466−1467.
(27) King, G. C.; di Giusto, D. A.; Wlassoff, W. A.; Giesebrecht, S.; Flening, E.; Tyrelle, G. D. *Hum. Mutat.* **2004**, *23*, 420−425.
(28) Mucic, R. C.; Herrlein, M. K.; Mirkin, C. A.; Letsinger, R. L. *J. Chem. Soc., Chem. Commun.* **1996**, 555−557.

Table 1. DNA Sequences of Hybrids

	polymer precursor (ratio)	sequence
I	poly**2**-poly**4** (17:10)	5′-T_3 ATC CTT ATC AAT ATT-3′
II	poly**2**-poly**4** (17:10)	5′-T_3 AAT ATT GAT AAG GAT-3′
III	poly**2**-poly**5** (17:10)	5′-T_3 ATC CTT ATC AAT ATT-3′
IV	poly**2**-poly**5** (17:10)	5′-T_3 AAT ATT GAT AAG GAT-3′
V	poly**2**-poly**4**-poly**5** (17:10:5)	5′-T_{10} ATC CTT ATC AAT ATT-3′
VI	poly**2**-poly**4**-poly**5** (17:5:5)	5′-T_{10} AAT ATT GAT AAG GAT-3′
VII	poly**2**-poly**5**-poly**4** (17:10:5)	5′-T_{10} TAA CAA TAA TCC CTC-3′
VIII	poly**2**-poly**5** (17:10)	5′-T_3 ATC CTT AGC AAT ATT-3′

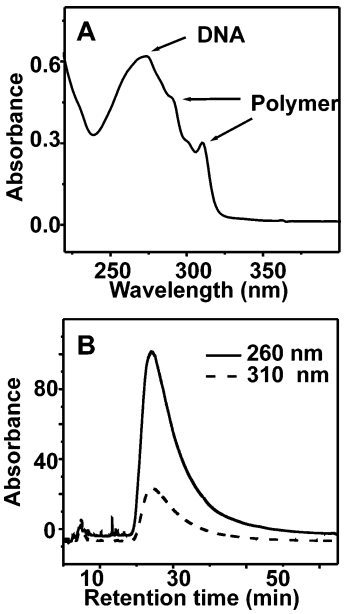

Figure 1. (A) UV−vis absorption spectrum of **Hybrid I** in water. (B) Ion-exchange HPLC chromatogram of purified **Hybrid I** monitored by UV−vis absorption at 260 nm (λ_{max} for DNA) and 310 nm (λ_{max} for diphenylacetylene). Both chromatograms show a single peak at the same retention time, indicating that DNA is indeed coupled to the polymer backbone.

(Scheme 1). DNA sequences and the length of each polymer block are given in Table 1.

Due to the hydrophilicity of the DNA block, the resulting polymer−DNA hybrids were soluble in aqueous media. The number of DNA strands attached to each hybrid was estimated from the UV−vis absorption spectra of the polymer conjugates in water (Figure 1A).[29] Ion-exchange HPLC was performed on purified **Hybrid I** (Figure 1B). One major peak at 25 min was observed at both 260 nm (λ_{max} of DNA) and 310 nm (λ_{max} of the diphenylacetylene spacer in the HPLC eluent), which further demonstrates that the oligonucleotides are indeed coupled to the polymer backbone. Preliminary results from capillary electrophoresis experiments indicate that our polymer−DNA hybrids are monodisperse.

The redox characteristics of the electrochemically active portion of the polymer can be tailored by using ferrocene

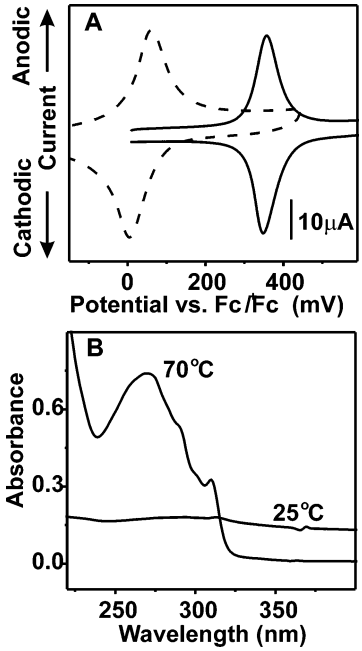

Figure 2. (A) Cyclic voltammograms of **Hybrid I** (dotted line) and **Hybrid III** (solid line) in CH_2Cl_2 with $[^nBu_4N]PF_6$ as electrolyte. The $E_{1/2}$ values are 30 mV and 350 mV (versus Fc/Fc^+) for **Hybrid I** and **Hybrid III**, respectively, as expected from the redox potentials of **4** and **5**. (B) Absorption spectra of a solution containing complementary polymer−DNA hybrids (**Hybrid I:Hybrid II**) above and below the DNA melting temperature, indicating that the aggregation is driven by DNA hybridization. The mixture of **Hybrid III** and **Hybrid IV** behaves the same way and shows similar temperature-dependent UV−vis absorption spectra.

derivatives with a variety of electron-donating or -withdrawing substituents. To demonstrate this capability, we chose two different norbornenyl-modified ferrocene derivatives, **4** and **5**, which exhibit $E_{1/2}$s separated by 320 mV. Electrochemical measurements were carried out on the hybrids by casting thin films of these materials on Au electrodes (see Supporting Information). Cyclic voltammetry of the resulting films in CH_2Cl_2 with $[^nBu_4N]PF_6$ as the electrolyte revealed stable and reversible waves associated with oxidation and reduction of the ferrocenyl blocks of the hybrid materials. The films are stable in the organic environment; multiple scans generated consistent results. As shown in Figure 2A, the $E_{1/2}$ value for **Hybrid I** was found to be 30 mV (versus Fc/Fc^+), while the $E_{1/2}$ of **Hybrid III** was 350 mV (versus Fc/Fc^+) (the formal potential value of Fc/Fc^+ in CH_2Cl_2 with $[^nBu_4N]PF_6$ is 0.46 V versus SCE).[30] These values are almost identical with the redox potentials observed for the corresponding monomers **4** and **5**.

DNA Recognition Properties of Diblock Copolymer−DNA Hybrids. As outlined in Table 1, complementary polymer−DNA hybrid structures (**Hybrid I** and **Hybrid II** from poly**2**-poly**4** and **Hybrid III** and **Hybrid IV** from poly**2**-poly**5**) were prepared for DNA recognition studies. When these complementary hybrids were mixed together in equal amounts (60 μM, 20 μL) in a PBS buffer (0.3 M NaCl, 10 mM phosphate, pH 7), extended polymer aggregates formed and precipitated from the solution in a few seconds. This observation demonstrates that the organic polymer portions of the hybrids do not inhibit the recognition properties of the DNA side chains. The UV−vis spectrum of the aggregate solution showed a significantly

(29) Based on the molar absorptivity of DNA at 287 nm and the diphenylacetylene spacer at 287 and 307 nm, we determined that there are, on average, five DNA strands per single polymer chain, which translates to ∼30% occupation of the 17 available DNA coupling sites on the poly**2** block. This value was calculated by first determining the polymer concentration based on the absorbance at 307 nm, which is only due to the polymer component and not the DNA. Knowing the polymer concentration and its molar absorptivity at 287 nm allowed us to subtract the polymers' absorbance at 287 nm from the total absorbance. The DNA concentration was determined from the remaining absorbance at 287 nm and the molar absorptivity value at 287 for the DNA sequences. The DNA concentration divided by the polymer concentration gives the average value of DNA per polymer.

(30) Connelly, N. G.; Geiger, W. E. *Chem. Rev.* **1996**, *96*, 877−910.

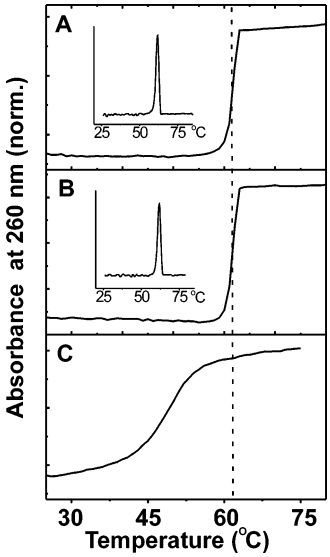

Figure 3. Thermal denaturation curves of networks formed from (A) **Hybrids I:II** and (B) **Hybrid III:IV**. Insets: the first derivatives of the thermal denaturation curves (fwhm = 2 °C). Two different block copolymer aggregates show similar melting transitions, indicating that the type of ferrocene would not affect the melting properties of DNA. Note that **Hybrids I** and **III** have the same DNA sequences, as do **Hybrids II** and **IV** (Table 1). Compared to the thermal denaturation curve for duplex DNA formed from unmodified oligonucleotides with the same sequence (C), the polymer aggregates show a much higher melting temperature and a sharper melting transition.

reduced signal at 260 nm and increased intensity at higher wavelengths due to scattering from the polymer aggregates (Figure 2B). Upon heating the aggregate solution to 70 °C, a temperature that is above the polymer-bound DNA's melting temperature (T_m = 62 °C), polymer−DNA hybrids can be redispersed in solution as evidenced by UV−vis spectroscopy (Figure 2B). The temperature dependence of aggregate formation indicates that the aggregates are indeed formed by sequence-specific DNA hybridization rather than nonspecific, hydrophobic interactions.

The thermal denaturation curves of these aggregates were obtained by monitoring their absorbance at 260 nm as a function of temperature (Figure 3). The block copolymer conjugates show unique DNA hybridization properties that differ from unmodified DNA. First, the aggregates formed from block copolymer−DNA (Figure 3A,B) show higher thermal stabilities (13 °C higher in melting temperatures) than unmodified duplex DNA (Figure 3C) of the same sequence at comparable concentrations. Similar high thermal stabilities have been observed in DNA dendrimers[3] and can be attributed to the presence of multiple DNA linkages which results in cooperative binding. This attribute suggests that the block copolymer−DNA hybrids might be useful as probes in DNA detection systems. Second, the aggregates formed from the hybrids show unusually sharp melting curves; the full widths at half-maximum (fwhm) for the first derivatives of the melting curves were ~2 °C (Figure 3A and B, inset). This is an unusual characteristic, as comparable "soft" nanostructure probes made of dendrimers apparently do not exhibit such a narrow melting transition.[3] The transitions observed for the novel probes reported herein are highly reminiscent of the sharp melting transition observed in the oligonucleotide-modified gold nanoparticle system, which has proven to be very useful in DNA diagnostics.[1,5,6]

Table 2. DNA Sequences Used in Polymer vs Molecular Probe Comparison

	precursor	sequence
Fc-DNA I	**6**	5′-T_3 ATC CTT ATC AAT ATT-3′
Fc-DNA II	**6**	5′-T_3 AAT ATT GAT AAG GAT-3′
polyDNA I	poly**2** (17-mer)	5′-T_3 ATC CTT ATC AAT ATT-3′
polyDNA II	poly**2** (17-mer)	5′-T_3 AAT ATT GAT AAG GAT-3′
DNA I	unmodified	5′-T_3 ATC CTT ATC AAT ATT-3′
DNA II	unmodified	5′-T_3 AAT ATT GAT AAG GAT-3′

Based on theoretical models, the local high density of DNA strands on our polymer backbone (as compared to free DNA in solution) appears to be crucial for inducing sharp thermal denaturation transitions in the resulting polymer−DNA hybrid.[31] As the oligonucleotide-modified gold nanoparticle probes offer high selectivity due to their sharp melting profiles,[7−9] the unique melting properties of the block copolymer−DNA hybrids point toward their potential use in high selectivity applications such as single-nucleotide polymorphism (SNP) detection.

Thermal Denaturation Studies of Polymer and Molecular Probes. We hypothesize that the unique melting profiles of our polymer probes, as well as that of DNA-modified gold nanoparticles, result from the presence of multiple DNA linkages in close proximity. Thus, we predicted that molecular probes would not exhibit such sharp melting transitions.

To test this prediction, we synthesized 5′-ferrocenyl labeled oligonucleotides (**Fc-DNA I** and **Fc-DNA II**) and homopolymer−DNA hybrids (**polyDNA I** and **polyDNA II**) (Table 2). These polymer hybrids were synthesized by coupling oligonucleotides to the polymer precursor, poly**2**, following a previous method.[12] The 5′-ferrocenyl labeled oligonucleotides (**Fc-DNA I** and **Fc-DNA II**) consist of a diphenylacetylene linker in addition to the ferrocenyl moiety (Figure 4A). The molecular probe was synthesized by converting one of our ferrocenyl monomer precursors[12] into a ferrocenyl alcohol with a three-carbon spacer. The (3-hydroxypropyl)ferrocene compound was then modified with a diphenylacetylene alcohol group following a synthetic strategy similar to that used for the synthesis of the norbornenyl monomer **2** (Scheme 2).[12] The resulting ferrocene derivative **11** was treated with chlorophosphoramidite and coupled to DNA in the same manner as the homopolymers. The diphenylacetylene functionality increased the retention time of the oligonucleotide sequence significantly during HPLC purification and absorbed strongly at 310 nm, allowing for easy purification and characterization of the molecular probe.

The similarity in the hydrophobic structure of the ferrocenyl molecular probe and the DNA side chains on the polymer allows for an accurate comparison of their melting properties. Primarily, the two types of probes differ in that the latter possesses multiple DNA strands in close proximity. Because any contribution of hydrophobicity[32] to the melting temperature should be approximately the same for both systems, comparing their thermal denaturation profiles should delineate whether the polymeric nature of the probe has a significant effect on DNA melting behavior.

Thermal denaturation curves were acquired using UV−vis spectroscopy as previously described. Two sets of hybridization

(31) Jin, R.; Wu, G.; Li, Z.; Mirkin, C. A.; Schatz, G. C. *J. Am. Chem. Soc.* **2003**, *125*, 1643−1654.
(32) Guckian, K. M.; Schweitzer, B. A.; Ren, R. X. F.; Sheils, C. J.; Tahmassebi, D. C.; Kool, E. T. *J. Am. Chem. Soc.* **2000**, *122*, 2213−2222.

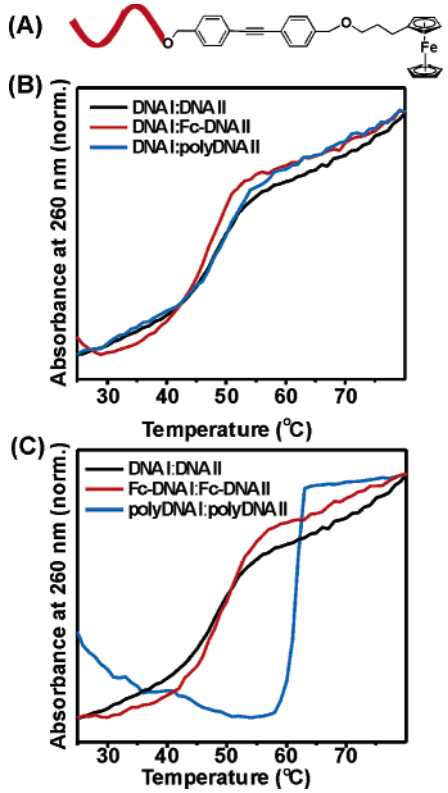

Figure 4. (A) Structure of **Fc-DNA**. (B) Thermal denaturation curves of **polyDNA II**, **Fc-DNA II**, and an unmodified oligonucleotide (**DNA II**) hybridized with a complementary, unmodified oligonucleotide (**DNA I**). (C) Thermal denaturation curves of **polyDNA**, **Fc-DNA**, and an unmodified oligonucleotide hybridized with their complementary analogue.

experiments were performed on each type of probe (**polyDNA** and **Fc-DNA**, Table 2). In the first set of experiments, each type of probe was hybridized with unmodified complementary oligonucleotide strands (**DNA I**). In the second set of experiments, each probe type was hybridized to its respective complementary probe, i.e., **Fc-DNA** with its complementary **Fc-DNA** and **polyDNA** with its complementary **polyDNA**. Interestingly, the melting profiles in the first data set are almost identical to one another as well as to the melting curve of the unmodified DNA duplex (Figure 4B). In contrast, in the second

Table 3. Thermal Stability Values

hybridization pair	melting temp (°C)	$<\Delta H_{VH}>$ (kcal/mol)	fwhm[a] (°C)
DNA I and **II**	49.0	99.7	9.4
DNA I and **Fc-DNA II**	50.3	96.3	10.4
DNA I and **polyDNA**[b] **II**	46.5	101	9.2
Fc-DNA I and **Fc-DNA II**	51.0	95.2	8.3
polyDNA[b] **I** and **polyDNA**[b] **II**	61.5	452	2.6

[a] fwhm: Full width at half-maximum of the first derivative ($d(\alpha)/d(1/T)$ vs T). [b] **polyDNA** was prepared from poly**2** (17-mer), and the average number of DNA attached to the polymer was determined to be five.

hybridization experiment, the **polyDNA I:polyDNA II** hybridization pair shows a greatly increased T_m (T_m = 61.5 °C, ΔT_m = 10 °C) and sharpened melting transition (fwhm = 2.6 °C) while the molecular probe-molecular probe (**Fc-DNA I:Fc-DNA II**) melting (T_m = 51 °C, fwhm = 8.3 °C) remains similar to that of unmodified DNA (T_m = 49 °C, fwhm = 9.4 °C) (Figure 4C). These results suggest that hydrophobicity does not contribute significantly to the melting properties of the attached oligonucleotides. Further, our experiments indicate that multiple DNA linkages do have a significant effect on DNA melting, but only when *both* strands of the hybridized duplex are bound to a structure containing multiple DNA strands. This conclusion could have large ramifications for probe optimization in chip-based assays, if one assumes that a DNA-modified surface acts as such a multiple-linked structure.

To quantify the difference in melting behavior, we performed simple thermodynamic calculations for each melting profile. Our calculations were a modification of two literature procedures[33,34] for calculating the van't Hoff mean enthalpic change, $<\Delta H_{VH}>$, which assumes a two-state transition model. There are limitations to this model, particularly in that it ignores the contributions of cooperativity (a multistate transition).[33,35] In addition, it does not account for the polymer−DNA duplexes forming larger aggregate structures. Nevertheless, the van't Hoff enthalpic calculation is a useful first-order approach for comparing the enthalpic difference involved in the dehybridization of probe-hybrid materials.

The values for $<\Delta H_{VH}>$ are listed in Table 3. With the exception of the **polyDNA I:polyDNA II** hybridization pair, all other hybridization pairs have $<\Delta H_{VH}>$ values of ap-

Scheme 2. Synthesis of the Molecular Probe Precursor

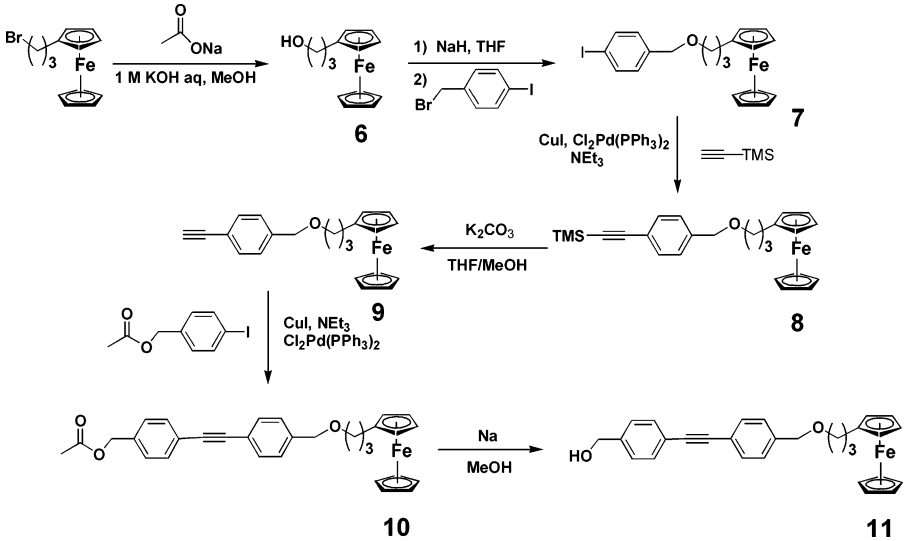

proximately 100 kcal/mol. Within experimental error it is difficult to deconvolute the effect of the polymer and molecular probes on the resulting duplexes where the complementary partner is either an unmodified DNA strand or a molecular probe. However, the **polyDNA:polyDNA** hybridization pair has a $<\Delta H_{VH}>$ value that is 4.5 times greater than any of the other hybridization pairs. This significant increase in thermal stability may be crucial to the success of assays that use genomic DNA with complex secondary structures. In addition, the melting ranges, listed as fwhm in Table 3, suggest that polymer probes should be able to discriminate SNPs better than molecular probes under stringent thermal conditions (or salt concentrations).[7−9] Thus, a comparison of melting profiles indicates that polymer probes such as the ones described herein could be better equipped for use in DNA detection than their molecular probe counterparts.

Syntheses of Triblock Copolymer−DNA Hybrids. Oligonucleotides have been modified with several redox-active compounds.[20,36−39] For example, Mucic et al. have developed 5′-ferrocenyl modified oligonucleotides as molecular probes for use in three-strand electrochemical detection assays.[28] Derivatizing ferrocene for covalent incorporation into oligonucleotides has also led to successful detection systems such as those reported by Yu et al.[17,24] and Kuhr et al.[21−23] One advantage of our polymer−DNA hybrid approach is the polyvalent cooperativity of the pendant DNA strands, which provide more specific discrimination of single-pair mismatches than analogous molecular probe systems (vide supra). The signaling amplification capabilities are also better for polymer−DNA hybrids, because polymers with larger blocks of labeling molecules can be synthesized, allowing for magnified detection signals. Additionally, the functional group tolerance and synthetic control that are native to ROMP polymerization enable us to develop a number of distinctly labeled probes quite easily. For example, by varying the molar ratio of two redox-active groups on the same polymer−DNA detection probe, numerous unique signatures based on not only the positions of the redox signals but also the amplitude ratios of these signals are possible. Such a system would have many advantages over molecular probe systems, particularly in multiplexing assays, because only a few electrochemical tags would be required to generate numerous barcodelike signatures, detectable by simple data-readout capabilities, using both identity and quantitative dimensions.

Based on our block copolymer strategy, in theory any DNA strand in a hybrid can be labeled with a unique electrochemical polymer tag. The detection of multiple DNA strands in a mixture can then be carried out by monitoring the electrochemical signal and referencing it to a particular probe associated with a target DNA sequence. However, the practical requirement that the different redox signals arising from the electrochemically active blocks be reasonably spaced apart to achieve complete signal discrimination only allows for the incorporation of approximately four different indicators in a detection system employing

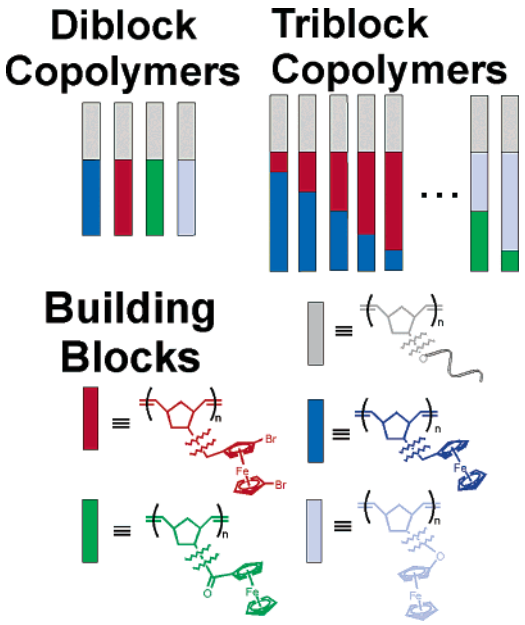

Figure 5. Schematic illustration of the triblock copolymer labeling strategy.

the diblock copolymer−DNA hybrid strategy. To increase the number of potential indicators, we synthesized triblock copolymers containing two different ferrocenyl derivatives, **4** and **5**. By adjusting the relative lengths of the two redox-active blocks one can generate several different tags corresponding to distinct combinations of the two electrochemically active monomers (Figure 5).[40] Triblock copolymer precursors were synthesized by polymerizing the DNA-modifiable diphenylacetylene monomer **2**, then adding ferrocene monomer **4**, and finally dibromoferrocene monomer **5** to the growing polymer chain. Each monomer was added to the polymerization mixture only after the previous type of monomer had been consumed. For proof-of-concept experiments, polymer precursors with approximately 2:1, 1:1, and 1:2 ratios of **4** and **5** were synthesized. Gel-permeation chromatographic (GPC) data for these polymers all showed a single peak, characteristic of a monodisperse sample, indicating that all three monomers are incorporated into a single polymer chain. The poly**2**-poly**4**-poly**5** precursors were then coupled to DNA to generate triblock copolymer−DNA **Hybrids V−VII** (Table 1). In the design of triblock copolymers, we employed a T_{10}-spacer instead of the T_3-spacer used for diblock copolymers to improve the water solubility of the final hybrids. As expected, triblock copolymer−DNA hybrids behave similarly to diblock copolymer hybrids as indicated by their UV−vis spectra and melting profiles (Figure 6).

Cyclic voltammograms of the triblock copolymer−DNA hybrids exhibit two distinct redox peaks at 30 and 350 mV (versus Fc/Fc^+) (Figure 7). Ratios of the peak current were found to be ∼ 2.7:1, 1:1, and 1:2.7 for **Hybrid V**, **Hybrid VI**, and **Hybrid VII**, respectively. Even though the peak current ratios are slightly different from the monomer ratios that we initially used (2:1, 1:1, and 1:2), these peak ratios and positions are consistent with those observed for the polymer precursors prior to DNA coupling. In fact, the cyclic voltammograms of the

(33) Marky, L. A.; Breslauer, K. J. *Biopolymers* **1987**, *26*, 1601−1620.
(34) Borer, P. N.; Dengler, B.; Tinoco, I., Jr.; Uhlenbeck, O. C. *J. Mol. Biol.* **1974**, *86*, 843−53.
(35) Marky, L. A.; Canuel, L.; Jones, R. A.; Breslauer, K. J. *Biophys. Chem.* **1981**, *13*, 141−149.
(36) Beilstein, A. E.; Grinstaff, M. W. *J. Organomet. Chem.* **2001**, *637−639*, 398−406.
(37) Hurley, D. J.; Tor, Y. *J. Am. Chem. Soc.* **1998**, *120*, 2194−2195.
(38) Weizman, H.; Tor, Y. *J. Am. Chem. Soc.* **2002**, *124*, 1568−1569.
(39) Hurley, D. J.; Tor, Y. *J. Am. Chem. Soc.* **2002**, *124*, 3749−3762.

(40) Consider the theoretical case of triblock copolymers with a maximum number of 5 repeating units per each electrochemically active block, distinct ratios which can be observed electrochemically would consist of the following: (0:5), (1:3), (1:4), (1:5), (2:3), (2:4), (2:5), (3:1), (3:2), (3:4), (3:5), (4:1), (4:2), (4:3), (4:5), (5:0), (5:1), (5:2), (5:3), (5:4), (5:5).

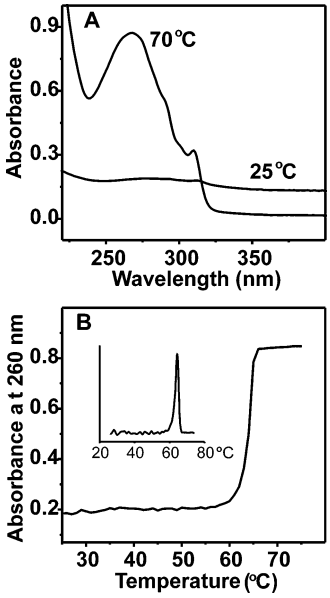

Figure 6. (A) Absorption spectra of triblock copolymer aggregates formed from **Hybrids V** and **VI** above and below the DNA melting temperature. (B) A thermal denaturation curve for the aggregates (Inset: first derivative).

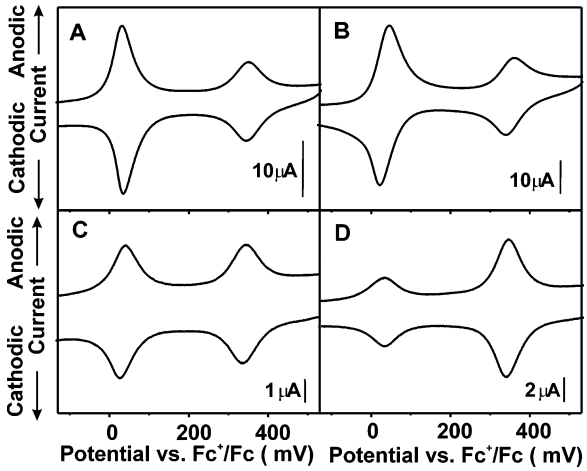

Figure 7. Cyclic voltammograms in CH_2Cl_2 with $[^nBu_4N]PF_6$ as electrolyte of (A) **Hybrid V**, a triblock copolymer−DNA with a 10:5 ratio of poly**4**:poly**5**, (B) polymer precursor of **Hybrid V**, (C) **Hybrid VI**, a triblock copolymer−DNA with a 5:5 ratio of poly**4**:poly**5**, and (D) **Hybrid VII**, a triblock copolymer−DNA with a 5:10 ratio of poly**4**:poly**5**. These triblock copolymer−DNA hybrids exhibit two distinct redox peaks with expected $E_{1/2}$ and peak intensity ratios. The detailed shape of the cyclic voltammograms caused by the diffusion-limited current and the charging current is dependent upon polymer film conditions. The cyclic voltammogram of the polymer precursor was obtained from a solution sample rather than a film cast on an electrode surface.

polymer-DNA hybrids and their polymer precursors are almost superimposable (Figure 7A,B). These results not only demonstrate the versatility of our synthetic methodology but also suggest the possibility of using the electrochemical signals as a type of barcode to tag many DNA targets present in a single sample solution.

DNA Detection Using Diblock Copolymer−DNA Hybrids. The block copolymer conjugates were utilized as DNA probes in a three-component sandwich-type electrochemical detection strategy (Scheme 3). In a typical experiment, a disulfide-modified oligonucleotide, ***a***, was immobilized on a freshly prepared Au electrode (0.5 × 2 cm^2) by applying 0.3 M PBS

Scheme 3. DNA Detection Based on Polymer−DNA Probes

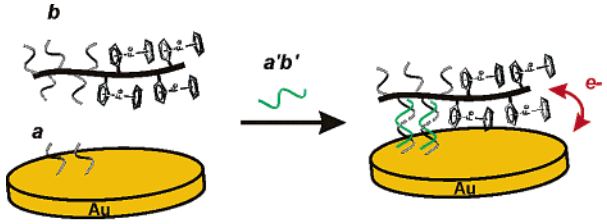

a 3'-CCT AAT AAC AAT-5'
b 3'-TTA TAA CTA TTC CTA T_3-5'
a'b' 5'-GGA TTA TTG TTA AAT ATT GAT AAG GAT-3'

solution of ***a*** (0.1 mM) to a part of the gold electrode (0.5 × 1 cm^2) for 16 h. Then, the electrode was washed with water and dipped in a 1 mM aqueous solution of mercaptohexanol for 5 min. This passivation procedure inhibits nonspecific binding of hybrid molecules to the gold electrodes. Finally, the electrode was washed with copious amounts of water and used for DNA detection studies.

To evaluate the performance of our polymer−DNA probes, synthetic target DNA (***a'b'***, 10 nM) and **Hybrid I** (1.2 nM) were cohybridized to ***a***-modified electrodes in PBS solution for 4 h at room temperature (Scheme 3). As a control experiment, another ***a***-modified electrode was treated with **Hybrid I** without target DNA under identical conditions. After washing the electrodes with PBS solution, alternating current (AC) voltammograms were acquired (Figure 8). The electrode treated with complementary target shows the desired redox signal due to **4** while the control sample generates no significant signal.

To test the sensitivity of the method described in Scheme 3, we have attempted to detect target at concentrations ranging from 10 nM to 1 pM. The ***a***-modified electrodes were treated with a series of target solutions (10 nM−1 pM) and polymer−DNA probe **Hybrid I** (2.4 nM) for 6 h. Then, AC voltammograms were obtained for each sample. As presented in Figure 8, we could easily detect target concentrations as low as 100 pM based on this detection method, which is an order of magnitude more sensitive than that reported by Yu et al. for their electrochemical molecular probe system.[17] When the target concentration was less than 100 pM, the signal level was indistinguishable from the background and was comparable to the signal intensity of the control electrode when only treated with **Hybrid I** (Figure 8, inset).

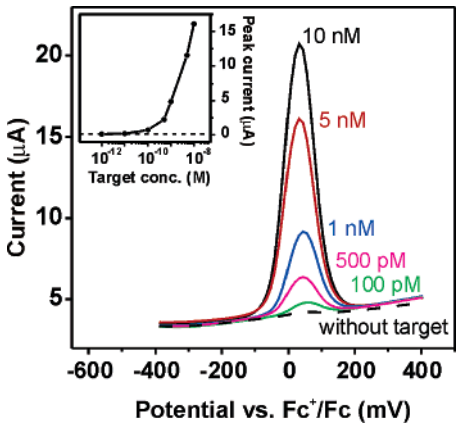

Figure 8. AC voltammograms in CH_2Cl_2 with $[^nBu_4N]PF_6$ as electrolyte for electrodes treated with different target concentrations. Inset: target concentration vs peak current. The horizontal dotted line is the peak current of the sample without the target DNA.

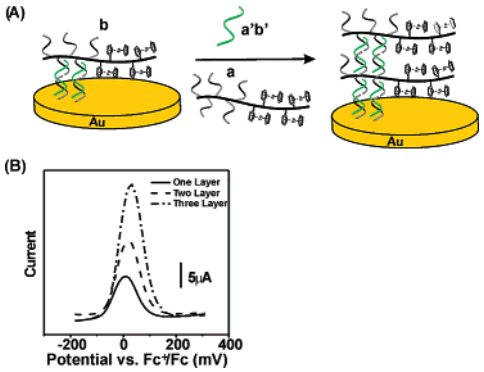

Figure 9. Signal amplification using polymer−DNA probes. (A) A scheme illustrating the addition of multiple layers to the electrode surface controlled by the recognition properties of DNA. (B) AC voltammograms in CH_2Cl_2 with $[^nBu_4N]PF_6$ as electrolyte of multilayer block copolymer−DNA hybrids assembled on a gold substrate.

The number of ferrocenyl groups bound to the gold electrodes was estimated to be 1.1×10^{13}, 3.4×10^{12}, and 5.2×10^{11} in the presence of 9.0×10^{12}, 9.0×10^{11}, and 9.0×10^{10} target strands (total sample volume = 1500 μL, area = 0.5 cm^2), respectively, using eq 1[41] where I_{avg} is the peak current, n is the number of electrons, T is the temperature, E_{ac} is the peak amplitude, f is the frequency, F is the Faraday constant, R is the gas constant, and N_{tot} is the total number of moles of redox active species corresponding to the peak.

$$I_{avg}(E_0) = 2nfN_{tot} \sin h(nFE_{ac}/RT)/\cos h(nFE_{ac}/RT) \quad (1)$$

It is noteworthy that the estimated number of ferrocenyl groups can be higher than the number of target DNA molecules present in solution. The higher ratio of ferrocenyl groups to target DNA is possible because each single polymer−DNA probe possesses about 10 ferrocenyl groups, on average. Thus the hybridization of one target DNA strand can, in principle, result in the attachment of 10 ferrocenyl groups to the electrode surface, thereby providing a form of signal amplification. Hence, detection methods based on these novel polymer−DNA probes can be more sensitive than methods utilizing oligonucleotides modified with only single ferrocenyl moieties, and the sensitivity of a detection system based on this approach should scale to some extent with the size of the block of redox groups.

Signal Amplification via Multilayering. Since our block copolymer-DNA hybrids possess multiple oligonucleotide side chains, in theory extra DNA strands are still available for further assembly of block copolymers after target hybridization if this latter process is less than 100% efficient or if the target concentration is less than polymer-bound DNA. To address the possibility of using these extra oligonucleotides for signal enhancement, a second and third layer of poly**4**-containing block copolymer−DNA hybrids (**Hybrid II** and **Hybrid I**, respectively) were assembled successively onto the electrode surface after the initial hybridization of target DNA and **Hybrid I** (Figure 9A and B). As the number of layers increased, the peak currents increased, showing that signal amplification via multilayering is indeed possible (Figure 9B). In these experiments, the sensitivity is increased proportionally to the number of layers. Thus, the magnitude of amplification will depend strongly on the number of ferrocenyl groups present in each of the hybrids used for building the successive layers.

(41) Sumner, J. J.; Weber, K. S.; Hockett, L. A.; Creager, S. E. *J. Phys. Chem. B* **2000**, *104*, 7449−7454.

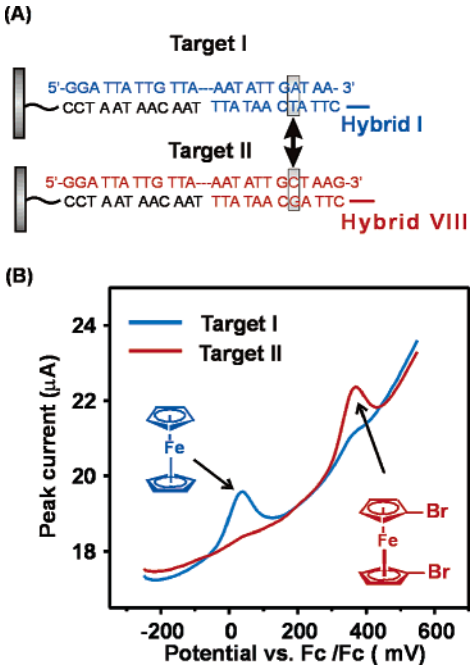

Figure 10. (A) Sequences of the target and probe DNAs used for dual-channel detection of a single-base mismatch. Note that **Hybrid I** and **Hybrid VIII** were prepared from **4** and **5**, respectively. (B) AC voltammograms in CH_2Cl_2 with $[^nBu_4N]PF_6$ as electrolyte for electrodes treated with either **Target I** or **Target II** in the presence of both detection probes. Only one major peak is shown at the expected potential for each case.

Detection of Single-Base Mismatches. In conventional DNA chip-based detection systems, two different color fluorophores are often used in each experiment for more accurate detection and to provide signal ratioing capabilities. In the DNA detection scheme reported herein, two types of hybrids with different ferrocenyl moieties can be used in a manner similar to the electrochemically based dual signaling procedure introduced by Yu et al.[17] The almost identical melting profiles of **Hybrid I:Hybrid II** and **Hybrid III:Hybrid IV** indicate that the nature of the ferrocenyl group does not significantly affect the melting properties of DNA (Figure 3A and B). This observation suggests that two different polymer−DNA probes synthesized from **4** and **5** can be utilized for the dual-channel detection of single-base mismatches. To evaluate the feasibility of this idea, two synthetic target DNA strands (**Target I** and **Target II** in Figure 10A) were prepared. **Target I** and **II** were designed to have only a single base difference at the position indicated by the arrow in Figure 10A. **Hybrid I** was synthesized as a signaling probe for **Target I**, and **Hybrid VIII** was synthesized as a signaling probe for **Target II**. In these experiments, we prepared two sample solutions (PBS, 1500 μL) containing (1) **Hybrid I**, **Hybrid VIII**, and **Target I** and (2) **Hybrid I**, **Hybrid VIII**, and **Target II**. Concentrations for polymer probes and target DNA were 1.2 nM and 10 nM, respectively, for both samples. Then, gold electrodes modified with capture DNA strands were immersed in the sample solutions and kept at 43 °C. After 4 h of incubation, the electrodes were washed with PBS buffer and dried with flowing N_2. Finally, AC voltammograms were obtained for each of the electrodes (Figure 10B). In each case, the redox signals attributable to the correspondingly matched signaling probes were the major peaks observed. The electrode

treated with the sample containing **Target I** produced a major signal at ~30 mV (versus Fc/Fc^+, Figure 10B), corresponding to the presence of ferrocenyl **Hybrid I** on the surface, and a trace signal at 350 mV, corresponding to the mismatched probe. The electrode treated with **Target II** produced a major signal at ~350 mV (versus Fc/Fc^+, Figure 10B), corresponding to the presence of dibromoferrocenyl **Hybrid VIII** on the surface, and a minor signal at 30 mV, corresponding to the mismatched probe. When the electrodes were incubated at room temperature, they show two strong redox peaks rather than a single one. Thus, selectivity in our strategy can easily be achieved using thermal stringency conditions. An increased hybridization temperature destabilizes only the mismatched probes, giving rise to one major redox peak that corresponds to the probe that is perfectly complementary to the target. These results demonstrate that the block copolymer probes can be used for the accurate detection of single base mismatches.

In summary, we have reported a new approach for preparing block-copolymer probes for DNA detection. Using this approach, we have prepared polymer−DNA hybrids with tailorable and well-controlled redox characteristics. These polymers possess the anticipated electrochemical properties that were designed into them but also unusual and unanticipated DNA hybridization properties. In particular, they exhibit stronger binding enthalpies and sharper melting profiles than the oligonucleotides from which they are made. These properties have allowed us to develop an electrochemical detection system that exhibits point-mutation selectivity and better target differentiation capabilities than those observed for single-oligonucleotide probes. Also, due to their strong binding constants, as reflected in increased T_m's, they should compete more effectively for target than conventional single-oligonucleotide probes. Finally, although only two types of probes have been evaluated for the proof-of-concept studies reported herein, in principle, a very large number of probes can be designed by systematically changing the length and composition of the redox-active blocks in the hybrid structures.

Acknowledgment. C.A.M. and S.T.N. acknowledge the National Science Foundation (Grant Nos. EEC-0118025 and DMR-0094347) and the AFOSR (Grant No. F49620-01-1-0303) for the financial support of this research. We thank Professors Irving M. Klotz and George C. Schatz, Drs. Richard Gurney and Jung Hyurk Lim, and Messrs. Shad Thaxton and Zhi Li for helpful discussions. J.M.G. and S.J.P. contribute equally to this work.

Supporting Information Available: Synthetic procedures and characterization data for polymer−DNA hybrids. Methods and data for hybridization and detection experiments. This material is available free of charge via the Internet at http://pubs.acs.org.

JA046931I